J Am Soc Nephrol 12: 107–113, 2001

Human Adolescent Nephronophthisis: Gene Locus Synteny with Polycystic Kidney Disease in Pcy Mice

HEYMUT OMRAN,* KARSTEN HÄFFNER,* SUSE BURTH,* CARMEN FERNANDEZ,† BERNARDO FARGIER,† AMINTA VILLAQUIRAN,† HANS-GERD NOTHWANG,† SUSANNE SCHNITTGER,§ HANS LEHRACH,‡ DAVID WOO,‖ MATTHIAS BRANDIS,* RALF SUDBRAK,‡ and FRIEDHELM HILDEBRANDT*

**University Children's Hospital, Freiburg University, Freiburg, Germany; †University Hospital Los Andes, Merida, Venezuela; ‡Max-Planck Institute for Molecular Genetics, Berlin, Germany; §University Hospital Groβhadern, Munich, Germany; and ‖University of California, Los Angeles, California.*

Abstract. In a large Venezuelan kindred, a new type of nephronophthisis was recently identified: Adolescent nephronophthisis (NPH3) is a late-onset recessive renal cystic disorder of the nephronophthisis/medullary cystic group of diseases causing end-stage renal disease at a median age of 19 yr. With the use of a homozygosity mapping strategy, the gene (*NPHP3*) was previously localized to chromosome 3q22 within a critical interval of 2.4 cM. In the current study, the *NPHP3* genetic region was cloned and seven genes, eight expressed sequence-tagged sites, and seven microsatellites were physically localized within the critical disease interval. By human-mouse synteny analysis based on expressed genes, synteny between the human *NPHP3* locus on chromosome 3q and the *pcy* locus on mouse chromosome 9 was clearly demonstrated, thus providing the first evidence of synteny between a human and a spontaneous murine renal cystic disease. By fluorescence *in situ* hybridization the chromosomal assignment of *NPHP3* to chromosome 3q21-q22 was refined. Renal pathology in NPH3 was found to consist of tubular basement membranes changes, tubular atrophy and dilation, and sclerosing tubulointerstitial nephropathy. This pathology clearly resembled findings observed in the recessive *pcy* mouse model of late-onset polycystic kidney disease. In analogy to *pcy*, renal cyst development at the corticomedullary junction was found to be an early sign of the disease. Through cloning of the NPH3 critical region and mapping of expressed genes, synteny between human NPH3 and murine *pcy* was established, thus generating the hypothesis that both diseases are caused by recessive mutations of homologous genes.

Nephronophthisis (NPH), an autosomal-recessive cystic kidney disorder, is a major genetic cause of chronic renal disease in children (1). Recently, we identified adolescent nephronophthisis (NPH3) as a novel type of NPH in a large consanguineous Venezuelan kindred. Applying a homozygosity mapping strategy, we localized the responsible gene (*NPHP3*) to a critical interval of 2.4 cM on chromosome 3q (2). Juvenile nephronophthisis (NPH1) and adolescent nephronophthisis (NPH3) share the same characteristic renal morphology, consisting of tubular basement membrane changes, tubular atrophy and dilation, sclerosing tubulointerstitial nephropathy, and cysts located predominantly at the corticomedullary junction. However, a gene locus for NPH1 (median age at end-stage renal disease [ESRD], 13.1 yr) was localized to 2q12 to q13, and the responsible gene *NPHP1* was found to be homozygously deleted in 70 to 80% of NPH1 patients (3,4). In contrast to NPH1, patients with NPH3 reach ESRD significantly later with a median age of 19 yr (range, 12 to 47 yr), thus rendering NPH3 the recessive renal cystic disease with the latest onset of ESRD (2). The best animal model for this disease seems to be the *pcy* mouse model for late-onset polycystic kidney disease, because inheritance is recessive, renal pathology resembles that of NPH3, and ESRD is reached in adult mice. To study whether both diseases might be homologous, we compared phenotypic and genetic findings in both diseases. By a physical mapping strategy, we cloned the *NPHP3* region, mapped several expressed genes, and were able to demonstrate by mapping data that *NPHP3* and *pcy* are syntenic. This is the first example of synteny between a human renal cystic disease and a spontaneous renal cystic mouse model. By fluorescence *in situ* hybridization, we were able to assign the chromosomal region of the human *NPHP3* locus to chromosome 3q21 to 3q22. In addition, by haplotype analysis in the large Venezuelan kindred with NPH3 (2), we identified two patients with NPH3 not reported previously. The identification of asymptomatic and symptomatic probands who carry the homozy-

Received April 17, 2000. Accepted June 1, 2000.
Correspondence to Dr. Heymut Omran, University Children's Hospital, Mathildenstrasse 1, 79106 Freiburg, Germany. Phone: 49-761-270-4301; Fax: 49-761-270-4533; E-mail: omran@kkl200.ukl.uni-freiburg.de
1046-6673/1201-0107
Journal of the American Society of Nephrology

gously affected haplotype enabled us to study the disease phenotype of NPH3 at different stages of the disease.

Materials and Methods

Physical Mapping

A set of 19 yeast artificial chromosomes (YAC) potentially residing at human chromosome 3q21 to q22 was derived from the information available in the public database of the Whitehead Institute (http://www-genome.wi.mit.edu). YAC clones were obtained from Centre d'Etude du Polymorphisme Humain (CEPH; Paris, France). Several polymorphic markers, sequence-tagged site (STS) markers, and expressed sequence-tagged site (EST) markers, presumably residing in the region of interest, were analyzed by PCR amplification individually for positivity with YAC clones by STS content mapping. Information for the examined markers concerning PCR primers, conditions, and location were retrieved through public databases (Whitehead [http://www-genome.wi.mit.edu], Cooperative Human Linkage Center [http://www.chlc.org], Genome database [http://www.gdb.org], Gene Map 99 [http://www.ncbi.nlm.nih.gov/genemap]). Inter-Alu PCR was performed using YAC clones 951a4 and 858b8 as templates (5). PCR products were used as probes for hybridization to screen the Peter de Jong P1 artificial chromosome (PAC) library (6). Bacterial artificial chromosome (BAC) libraries CEPH B and Research Genetics RB (Research Genetics, Huntsville, AL) were screened for STS content. BAC/PAC clones were tested by STS content mapping with the above markers. BAC/PAC ends were sequenced, and PCR primers for clone-end markers were generated. For STS content mapping, one individual colony was picked for each YAC, PAC, or BAC clone. One colony was suspended in 200 μl of sterile water. Ten μl of each sample were dried in a microtiter plate, followed by one negative control (water for template) and one positive control (10 to 30 ng of genomic DNA of a healthy individual). PCR was performed with dry template, 6 to 18 pmol of primers, 0.2 mM each dATP, dCTP, dGTP, and dTTP, 10 mM Tris-HCl (pH7.3), 50 mM KCl, 0.001% gelatin (w/vol), and 0.3 U of *Thermus aquaticus* DNA polymerase (Perkin-Elmer Cetus, Norwalk, CT). Amplification was carried out with denaturation at 94°C for 30 s, annealing at 53 to 60°C for 30 s, extension at 72°C for 60 s, and 32 cycles. PCR products were separated by electrophoresis in a 1% agarose gel. The gels were stained with ethidium bromide and photographed. Each result was confirmed at least once. BAC/PAC ends were directly sequenced using the Big dye sequencing system (ABI-377, Perkin-Elmer Cetus), and PCR primers for clone-end markers were generated.

Human-Mouse Synteny Analysis

On the basis of the physical mapping data obtained with the studies described above and on the basis of physical mapping data from the Mouse Genome Project (data obtained from http://www.jackson.org), we performed a human-mouse synteny analysis using for DNA sequence comparison the BLAST-N subroutine (7). The *pcy* locus has been mapped to mouse chromosome 9 and is flanked by markers D9Mit16 and D9Mit24 (8). Physical data for the centromeric part of this critical region are available from the Whitehead YAC-contig WC9.35 (http://www-genome.wi.mit.edu). We used all mouse STS and EST sequences of that contig and performed BLAST-N analysis. If no sequence similarity to any human EST/gene was obtained, we conducted a BLAST-N analysis to identify a murine EST cluster. This EST cluster was again used for BLAST analysis to identify homologous human EST or genes.

Fluorescence In Situ Hybridization

Metaphases were harvested after direct preparations of short-term cultures (24 to 48 h) of phytohemagglutinin-stimulated normal peripheral blood lymphocytes. Methods of cell culture, chromosome preparation, and staining by a modified GAG banding technique have been described previously (9,10). Chromosomal bands were classified according to the International System for Cytogenetic Nomenclature (ISCN, 1995). After fixation in methanol:acetic acid 3:1, the cells were air dried on glass slides and frozen at −20°C for at least 1 d. PAC/BAC DNA of clones RB815E10, 874N07, 544P15, 967G23, 156M15, and 286D11, which are located within the critical genetic *NPHP3* region (for exact location of the probes, see Figure 1) was labeled with Texas Red (Molecular Probes, Göttingen, Germany) using a nick translation kit (Vysis, Bergisch Gladbach, Germany). Ten ng of labeled DNA was dissolved in 10 μl of hybridization solution consisting of 50% formamide, 10% dextran sulfate, 1 × SSC, 500 ng of Cot-1 DNA, and 5 μg of sonicated salmon sperm DNA and then denatured at 95°C for 5 min. Slides with metaphase spreads of normal human controls were denatured in 70% formamide/2 × SSC at 72°C for 3 min on a heating plate and subsequently passed through a graded ethanol series. The slides were counterstained with 4,6-diamino-2-phenylindol (2 mg/ml) and mounted in anti-fade solution (90% glycerol, 10% phosphate-buffered saline, 1 mg/ml phenylenediamine). Metaphases were analyzed using Zeiss Axiophot epifluorescence microscope equipped with filter combination 1 according to Pinkel and a cooled charge-coupled device camera (Metasystems, Altlussheim, Germany) was used. TexasRed and 4,6-diamino-2-phenylindol fluorescence were recorded separately as gray-scale images by changing the excitation wave length only while the beam splitter and emission filter remained in position. The images were then pseudocolored and were merged using a digital image analysis software program (ISIS, Metasystems).

Clinical Studies

In the large Venezuelan kindred with NPH3 (2), blood samples from 13 probands who had not been studied previously were obtained on the basis of informed consent. Haplotype analysis with microsatellites from the *NPHP3* region was performed as described previously (2). All probands were studied by measurement of serum creatinine, hemoglobin level, and urinalysis. Renal ultrasound was performed in probands ID202 and ID213 carrying the homozygously affected haplotype diagnostic for NPH3. In proband ID202, maximum urine concentration capacity was tested by a 12-h water deprivation test. Serum and urine osmolarity were measured at 0 and 12 h of the test. In proband ID213, who presented in chronic renal failure, renal biopsy was performed and evaluated using standard histopathology staining procedures.

Results

Physical Mapping

We generated a complete YAC contig spanning the whole critical region of NPH3, thereby cloning the *NPHP3* critical genetic region (Figure 1, a and b). The critical disease interval is flanked by the centromeric marker D3S1292 and the telomeric marker D3S1238. The maximum physical distance for the two markers that flank the *NPHP3* region as defined by the combined length of clones 951a4 and 858b8 is 3.3 Mb. We thereby restricted the physical interval for *NPHP3* to less than 3.3 Mb (Figure 1b). We physically localized seven expressed genes (*ACPP* [phosphatase, prostate-specific acid], *TOPB1*

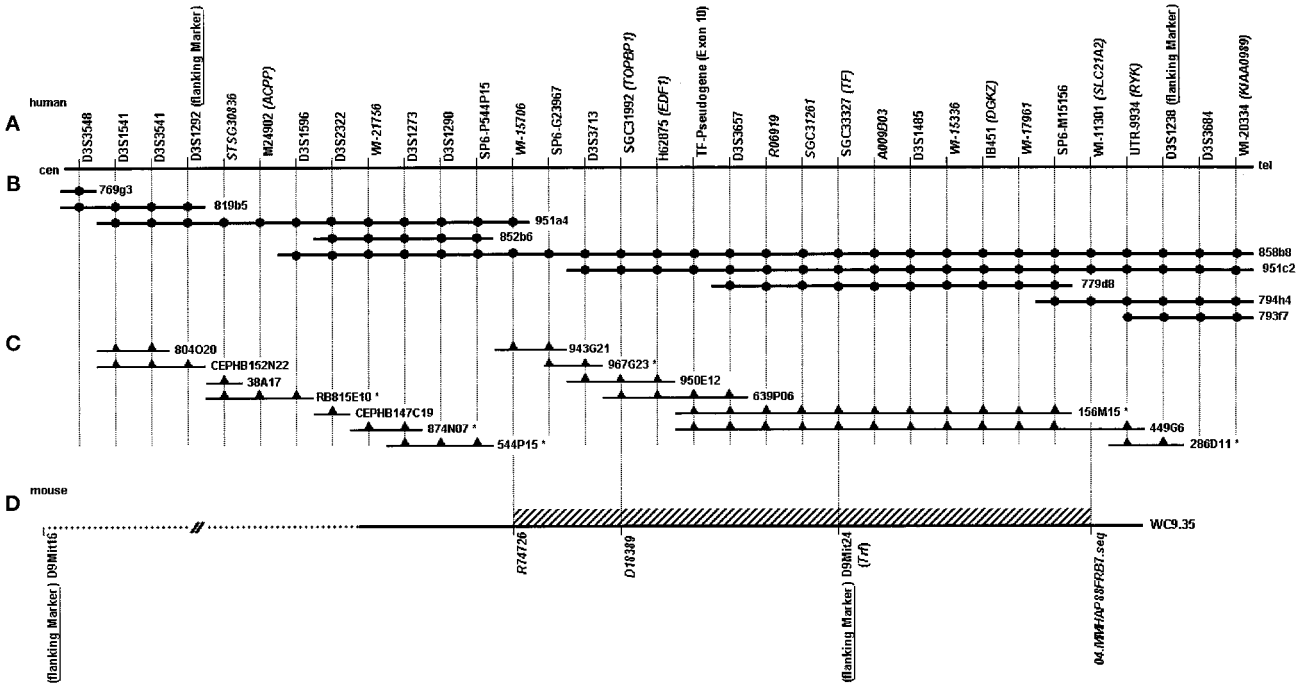

Figure 1. Physical map of the human *NPHP3* (a through c) and the mouse *pcy* (d) loci. (a) Polymorphic markers and sequence-tagged sites in the *NPHP3* region. Flanking markers are D3S1292 and D3S1238. Gene symbols are given in parenthesis. Expressed sequence-tagged sites (EST) are shown in italics. (b) Complete yeast artificial chromosomes (YAC) contig generated in the region. Sequence-tagged site (STS) content for markers in (a) is indicated by vertical lines and dots on YAC clones. (c) PAC and BAC in the region. STS content for markers in (a) is indicated by vertical lines and triangles. PAC or BAC with asterisks were studied by fluorescence *in situ* hybridization (FISH) and are located on human chromosome 3q21 to q22. (d) Whitehead YAC contig (WC9.35) on mouse chromosome 9 of the *pcy* locus with EST markers showing homology to genes identified in the human *NPHP3* region. The minimal syntenic region of *NPHP3* and *pcy* is shown hatched. The centromeric (cen) to telomeric (tel) orientation is indicated.

[topoisomerase (DNA) II binding protein], *EDF1* [endothelial differentiation-related factor 1], *TF* [transferrin], *DGKZ* [diacylglycerol kinase-zeta], *SLC21a2* [prostaglandin transporter, PGT], *RYK* [receptor-like tyrosine kinase]), eight EST, seven microsatellites, and three STS markers within the critical disease interval for which previously no physical location was known.

Human-Mouse Synteny Analysis

Human-mouse synteny analysis was performed on the basis of expressed genes localized to the YAC/PAC/BAC contig generated. Four murine EST residing on Whitehead YAC contig WC9.35 within the *pcy* critical disease interval showed a very high degree of sequence similarity with human genes/EST of the critical region of *NPHP3* (see Figure 1d). The order of the four genes/EST was found to be conserved between human and mouse. This high degree of continuous sequence similarity gives evidence that human *NPHP3* and murine *pcy* map to syntenic genetic regions (Figure 1). For results of BLAST analysis, see Table 1.

Fluorescence In Situ Hybridization

Fluorescence in situ hybridization (FISH) analysis with clones RB815E10, 874N07, 544P15, 967G23, 156M15, and 286D11 that are located within the critical disease interval of *NPHP3* (Figure 1) revealed positive signals only for human

Table 1. Results of sequence similarity analysis using murine EST and genes located in the vicinity of the pcy locus[a]

Mouse EST or Gene	Homologous Human EST or Gene[b]	Sequence Identity
D9Mit24, trf (transferrin)	TF (transferrin)	94/115 (81%)
04.MMHAP88FRB7.seq	SLC21a2 (prostaglandin transporter)	111/127 (87%)
D18389, EST-cluster Mm. 1687	TOPBP1	280/327 (85%)
R74726	EST cluster Hs. 103379 (WI-15706)	169/191 (88%)

[a] EST, expressed sequence-tagged site.
[b] All human homologous EST and genes that were identified are located within the critical region of *NPHP3* (see Figure 1), demonstrating synteny of the human *NPHP3* and the murine *pcy* locus.

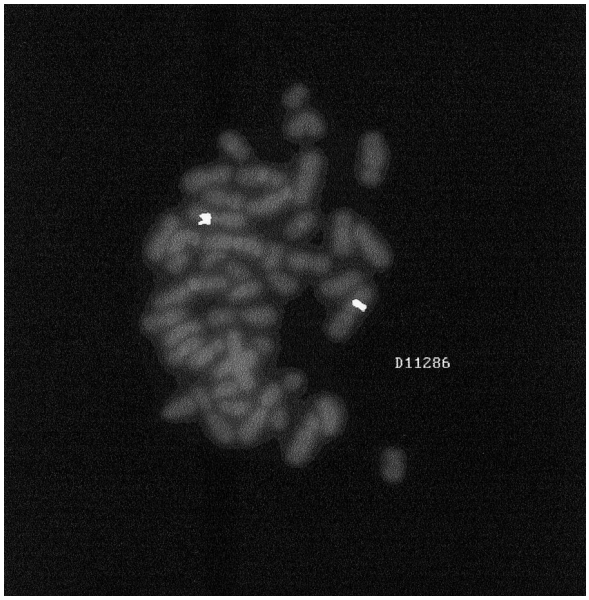

Figure 2. FISH mapping of PAC clone 286D11 (alias D11286) on human chromosome 3q21 to q22.

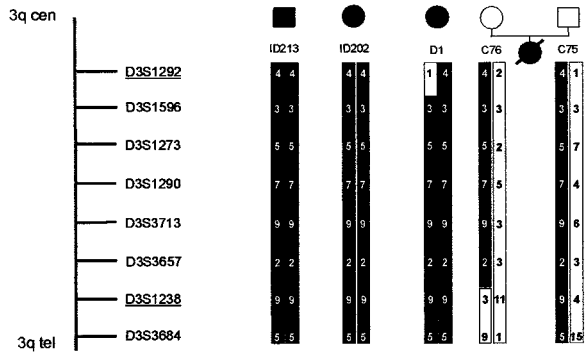

Figure 3. Haplotype analyses of new probands ID213 and ID202 from the large Venezuelan adolescent nephronophthisis (NPH3) kindred. Note that both probands homozygously share the same haplotype that is associated with the affected status of the Venezuelan kindred studied (2). For comparison, haplotypes of three previously reported individuals are shown, one affected proband and one obligate carrier, in whom recombinations for markers D3S1292 and D3S1238, respectively, define the critical region of NPH3 (underlined). The centromeric (cen) to telomeric (tel) orientation is indicated.

chromosome 3q21 to q22. To illustrate these data, the results from FISH analysis using PAC 286D11 is shown in Figure 2.

Clinical Studies

From the 13 probands studied, we identified 2 probands with a homozygously affected haplotype diagnostic for NPH3 (Figure 3). Laboratory investigations and haplotypes for the other 11 probands were normal. Proband ID202 was a 12-yr-old girl without any clinical complaints. Laboratory investigations including maximum urine concentration capacity were normal. Ultrasound of her kidneys revealed multiple small cysts measuring approximately 0.5 cm in diameter at the corticomedullary junction. The male proband ID213 presented with polyuria and loss of appetite at the age of 27 yr. His serum creatinine was 18.8 mg/dl. Within 1 mo of clinical presentation, renal replacement therapy had to be implemented. Ultrasound examination of the kidney revealed multiple cysts in both kidneys. The cysts were predominantly located at the corticomedullary junction but also elsewhere in the kidney (Figure 4, a and b). Histology showed typical findings for NPH3 consisting of tubular basement membranes changes with segments of thickening, thinning, folding and a multilayered appearance, tubular atrophy and dilation, mononuclear infiltrates and diffuse interstitial fibrosis, and concentric periglomerular fibrosis with thickening of Bowman's capsule (Figure 4d). Ultrasound findings and histologic findings in patient ID213 were compared with findings from macroscopic and microscopic anatomy in the pcy mouse (Figure 4).

Discussion

NPH3 was only recently identified as a novel type of NPH in a large Venezuelan inbred kindred (2). ESRD is reached in NPH3 at a median age of 19 yr, indicating that this disease has a late onset of ESRD, when compared with other recessive renal cystic diseases such as infantile and juvenile NPH and autosomal-recessive polycystic kidney disease (11–13). We previously localized the gene locus (*NPHP3*) of NPH3 to a 2.4-cM interval on chromosome 3q applying a homozygosity mapping strategy in a large Venezuelan kindred (2).

To identify the responsible gene *NPHP3*, we cloned the critical *NPHP3* region in a complete YAC and partial PAC/BAC contig and physically localized several genes/EST within the region of interest. The maximum length of the critical *NPHP3* region is less than 3.3 Mb and corresponds to the combined length of clones 951a4 and 858b8. By FISH analysis using PAC/BAC clones evenly distributed within the critical region of *NPHP3*, we cytogenetically localized the gene locus to chromosome 3q21 to q22 (Figure 2). On the basis of these human physical mapping data of the critical *NPHP3* region, a human-to-mouse synteny analysis was performed and allowed definition of synteny for *NPHP3* and a genetic region on mouse chromosome 9 (Figure 1). How far the area of synteny reaches centromeric toward human chromosome 3q21 or murine chromosome 9tel, respectively, cannot be discerned because no additional mouse physical data are available for that region. It is interesting that the genetic region on mouse chromosome 9 contains the polycystic kidney disease (*pcy*) locus, which was previously mapped to mouse chromosome 9 flanked by D9Mit16 and D9Mit24 (8). Thus, we demonstrate synteny between the human *NPHP3* and the murine cystic kidney disease locus *pcy* (Figure 1). To our knowledge, this is the first report of synteny between a human and a spontaneous mouse cystic kidney disease locus. Among recessive mouse models of renal cystic disease, pcy is the mouse model with the most slowly progressing adult-type form of polycystic kidney disease (14,15), thus resembling the late manifestation of NPH3. Disease traits in pcy and NPH3 share the same autosomal-recessive inheritance pattern. By back-crossing the affected *pcy* gene to different mouse strains, a variation of the severity

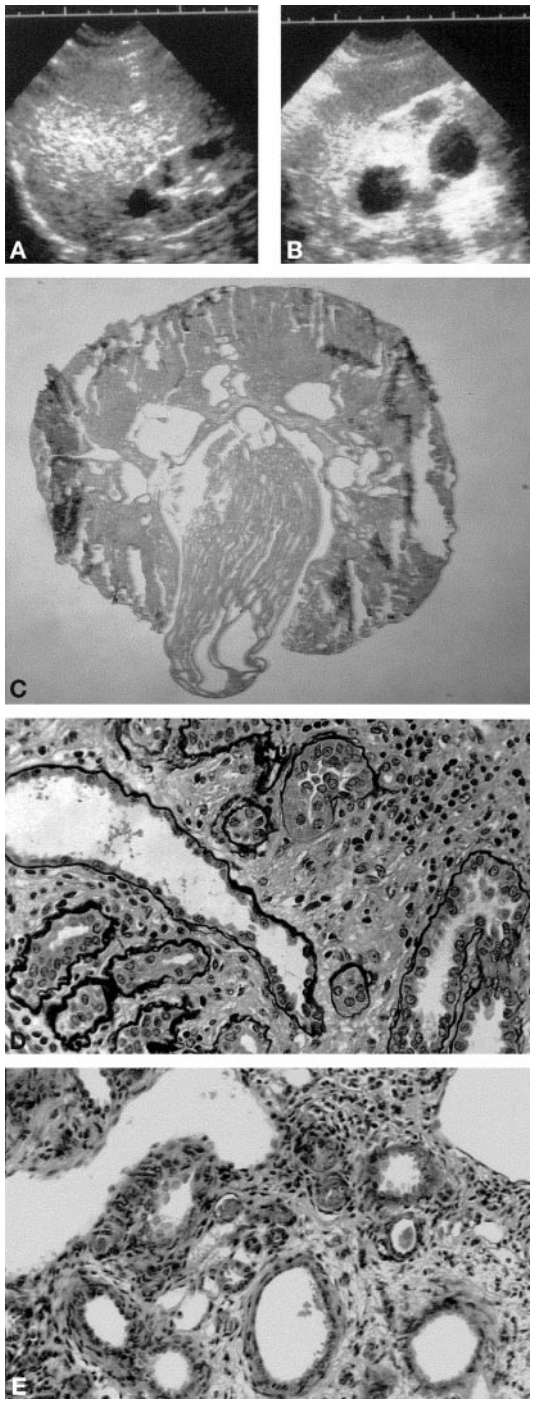

Figure 4. Renal ultrasound of proband ID213 showing a right kidney (A) with a length of 7.6 cm and a left kidney (B) measuring 8.3 cm. Kidneys have increased echogenicity and multiple cysts ranging in size from 0.2 to 2.0 cm in diameter. (C) Cross section of a 2-wk-old pcy mouse showing cysts located predominantly at the corticomedullary junction and in the medulla. (D) Silver-methenamine trichrome staining of a renal biopsy of proband ID213 with typical findings for NPH3 consisting of tubular basement membranes changes with segments of thickening, thinning, folding and a multilayered appearance, tubular atrophy and dilation, mononuclear infiltrates, and diffuse interstitial fibrosis. (E) Periodic acid-Schiff staining of renal specimen of a 2-mo-old pcy mouse exhibiting similar findings as observed in NPH3, consisting of tubular atrophy and dilation, mononuclear infiltrates, and diffuse interstitial fibrosis.

of the pcy phenotype in relation to different genetic backgrounds was noted (16). Subsequently, two modifier loci on mouse chromosomes 4 and 16 were identified by linkage analysis (17). The presence of modifier genes could also serve to explain the wide age range (12 to 47 yr) of ESRD observed in NPH3. Comparison of NPH3 and pcy revealed several phenotypic similarities, including (*1*) mode of inheritance, (*2*) late disease manifestation, (*3*) renal cyst location at the corticomedullary junction, (*4*) lack of extrarenal disease manifestations such as hepatic disease, and (*5*) histology (see also Table 2). There was, however, a dissimilarity with respect to renal enlargement and cerebral vascular aneurysms present in pcy but not in NPH3.

Because all reported patients with NPH3 presented already in ESRD, only little is known about the disease before renal failure. Therefore, we screened new relatives of the large Venezuelan kindred with NPH3, reported previously (2). We identified a 12-yr-old girl with no clinical symptoms, who carries a homozygously affected haplotype for markers from the *NPHP3* region (Figure 3). This enabled us to study the disease phenotype of NPH3 before renal failure. Laboratory investigations including urine concentration capacity were normal. Because in ID202 renal sonography showed cysts at the corticomedullary junction, renal cyst development at the corticomedullary junction seems to be an early sign of NPH3 in this proband. The other proband who was diagnosed as having NPH3 was 27 yr old and presented with clinical and laboratory findings of chronic renal failure (Figure 3). Ultrasound of his kidneys showed multiple cysts throughout the entire kidney but predominantly located at the corticomedullary junction (Figure 4). In pcy, cysts tend to develop primarily at a similar site in the kidney (Figure 4). Takahashi *et al.* (15) noted in DBA/2-pcy/pcy mice by 4 wk of age a well-delineated cyst in the outer portion of the inner medulla in almost every sample examined, and in the latest stages of the disease (30 wk and older) the whole kidney was enlarged and dominated by cysts. Therefore, early cyst development seems to be an early sign of NPH3 and pcy. It is interesting that histopathologic changes observed in NPH3 and pcy show similarities (Figure 4, d and e), consisting of predominant dilation of distal tubules and collecting ducts, sporadic dilation of Bowman's capsule, and interstitial inflammatory infiltrates causing a chronic sclerosing tubulointerstitial nephropathy (2,15). In addition, tubular basement membrane changes with local attenuation, thickening, and multilayering, which are supposed to be characteristic findings in adolescent and juvenile NPH, can also be observed in pcy mice (2,15,18,19).

On the basis of genetic and phenotypic findings, NPH3 and murine pcy most likely are caused by recessive mutations of homologous genes. This will help to accelerate gene identification of NPH3 and pcy because the search for the responsible genes should be focused to the critical genetic region that overlaps in both diseases, which is flanked by D3S1292 and SGC3327 (*TF*). Considering all EST and genes localized within this interval, only *EDF1* and *TOPB1* show a broad expression pattern, including kidney similar to the expression pattern of *NPHP1* (20), thus rendering them potential candi-

Table 2. Comparison of clinical, pathological, and genetic findings of adolescent NPH and polycystic kidney disease in mice (pcy)[a]

	Adolescent NPH	Polycystic Kidney Disease (pcy)
Inheritance	Autosomal recessive	Autosomal recessive
Manifestation of renal failure	Late (median age, 19 yr)	Late (adult mice)
Range of age at renal failure	Wide range (12 to 47 yr)	Wide range depending on genetic background
Renal cyst location	Predominantly at the corticomedullary junction	In the beginning at the corticomedullary junction, later throughout the entire kidney
Kidney size	Normal or reduced	Enlarged
Extrarenal disease manifestation	Not known	Cerebral vascular aneurysms in 12%
Histology	Tubular basement membrane changes, tubular dilation and atrophy, sclerosing tubulointerstitial nephropathy	Tubular basement membrane changes, tubular dilation and atrophy, sclerosing tubulointerstitial nephropathy

[a] NPH, nephronophthisis.

date genes (http://www.ncbi.nlm.nih.gov/UniGene). If homology of NPH3 and pcy is confirmed by gene identification, this will, in addition, have clinical implications, because intervention studies in pcy mice have demonstrated beneficial effects by modification of protein intake and administration of methylprednisolone (21–24).

Acknowledgments

H.O. and F.H. were supported by a grant of the German Research Foundation (DFG Om 6/1-1; DFG Hi 381/3-3) and by a grant from the Zentrum Klinische Forschung, Freiburg (ZKF-A1). The excellent technical assistance of Martina David is gratefully acknowledged.

References

1. Hildebrandt F: Nephronophthisis. In: Pediatric Nephrology, edited by Avner E, Barrat T, Harmon W, Baltimore, Williams & Wilkins, 1999, pp 453–458
2. Omran H, Fernandez C, Jung M, Häffner K, Fargier B, Villaquiran A, Waldherr R, Gretz N, Brandis M, Rüschendorf F, Reis A, Hildebrandt F: Identification of a new gene locus for adolescent nephronophthisis, on chromosome 3q22 in a large Venezuelan pedigree. *Am J Hum Genet* 66: 118–127, 2000
3. Hildebrandt F, Otto E, Rensing C, Nothwang HG, Vollmer M, Adolphs J, Hanusch H, Brandis M: A novel gene encoding an SH3 domain protein is mutated in nephronophthisis type 1. *Nat Genet* 17: 149–153, 1997
4. Saunier S, Calado J, Heilig R, Silbermann F, Benessy F, Morin G, Konrad M, Broyer M, Gubler MC, Weissenbach J, Antignac C: A novel gene that encodes a protein with a putative src homology 3 domain is a candidate gene for familial juvenile nephronophthisis. *Hum Mol Genet* 6: 2317–2323, 1997
5. Nelson DL, Ledbetter SA, Corbo L, Victoria MF, Ramirez-Solis R, Webster TD, Ledbetter DH, Caskey CT: Alu polymerase chain reaction: A method for rapid isolation of human-specific sequences from complex DNA sources. *Proc Natl Acad Sci USA* 86: 6686–6690, 1989
6. Ioannou PA, Amemiya CT, Garnes J, Kroisel PM, Shizuya H, Chen C, Batzer MA, de Jong PJ: A new bacteriophage P1-derived vector for the propagation of large human DNA fragments. *Nat Genet* 6: 84–89, 1994
7. Altschul SF, Madden TL, Schaffer AA, Zhang J, Zhang Z, Miller W, Lipman DJ: Gapped BLAST and PSI-BLAST: A new generation of protein database search programs. *Nucleic Acids Res* 25: 3389–3402, 1997
8. Nagao S, Watanabe T, Ogiso N, Marunouchi T, Takahashi H: Genetic mapping of the polycystic kidney gene, pcy, on mouse chromosome 9. *Biochem Genet* 33: 401–412, 1995
9. Fonatsch C, Schaadt M, Kirchner H, Diehl V: A possible correlation between the degree of karyotype aberrations and the rate of sister chromatid exchanges in lymphoma lines. *Int J Cancer* 26: 749–756, 1980
10. Stollmann B, Fonatsch C, Havers W: Persistent Epstein-Barr virus infection associated with monosomy 7 or chromosome 3 abnormality in childhood myeloproliferative disorders. *Br J Haematol* 60: 183–196, 1985
11. Haider NB, Carmi R, Shalev H, Sheffield VC, Landau D: A Bedouin kindred with infantile nephronophthisis demonstrates linkage to chromosome 9 by homozygosity mapping. *Am J Hum Genet* 63: 1404–1410, 1998
12. Hildebrandt F, Strahm B, Nothwang HG, Gretz N, Schnieders B, Singh-Sawhney I, Kutt R, Vollmer M, Brandis M: Molecular genetic identification of families with juvenile nephronophthisis type 1: Rate of progression to renal failure. APN Study Group. Arbeitsgemeinschaft fur Padiatrische Nephrologie. *Kidney Int* 51: 261–269, 1997
13. Zerres K, Rudnik-Schoneborn S, Deget F, Holtkamp U, Brodehl J, Geisert J, Scharer K: Autosomal recessive polycystic kidney disease in 115 children: Clinical presentation, course and influence of gender. Arbeitsgemeinschaft fur Padiatrische, Nephrologie. *Acta Paediatr* 85: 437–445, 1996
14. Takahashi H, Ueyama Y, Hibino T, Kuwahara Y, Suzuki S, Hioki K, Tamaoki N: A new mouse model of genetically transmitted polycystic kidney disease. *J Urol* 135: 1280–1283, 1986
15. Takahashi H, Calvet JP, Dittemore-Hoover D, Yoshida K, Grantham JJ, Gattone VH: A hereditary model of slowly progressive polycystic kidney disease in the mouse. *J Am Soc Nephrol* 1: 980–989, 1991
16. Nagao S, Hibino T, Koyama Y, Marunouchi T, Konishi H, Takahashi H: Strain difference in expression of the adult-type polycystic kidney disease gene, pcy, in the mouse. *Jikken Dobutsu* 40: 45–53, 1991
17. Woo DD, Nguyen DK, Khatibi N, Olsen P: Genetic identification of two major modifier loci of polycystic kidney disease progression in pcy mice. *J Clin Invest* 100: 1934–1940, 1997

18. Zollinger HU, Mihatsch MJ, Edefonti A, Gaboardi F, Imbasciati E, Lennert T: Nephronophthisis (medullary cystic disease of the kidney): A study using electron microscopy, immunofluorescence, and a review of the morphological findings. *Helv Paediatr Acta* 35: 509–530, 1980
19. Nagao S, Koyama Y, Takahashi H: Specific changes in the basement membrane of the proximal tubules in the murine polycystic kidney detected by the novel anti-basement membrane monoclonal antibody D28. *Jikken Dobutsu* 43: 511–519, 1994
20. Otto E, Kispert A, Schätzle S, Lescher B, Rensing C, Hildebrandt F: Nephrocystin: Gene expression and sequence conservation between human, mouse and *Caenorhabditis elegans*. *J Am Soc Nephrol* 11: 270–283, 2000
21. Aukema HM, Ogborn MR, Tomobe K, Takahashi H, Hibino T, Holub BJ: Effects of dietary protein restriction and oil type on the early progression of murine polycystic kidney disease. *Kidney Int* 42: 837–842, 1992
22. Tomobe K, Philbrick D, Aukema HM, Clark WF, Ogborn MR, Parbtani A, Takahashi H, Holub BJ: Early dietary protein restriction slows disease progression and lengthens survival in mice with polycystic kidney disease. *J Am Soc Nephrol* 5: 1355–1360, 1994
23. Tomobe K, Philbrick DJ, Ogborn MR, Takahashi H, Holub BJ: Effect of dietary soy protein and genistein on disease progression in mice with polycystic kidney disease. *Am J Kidney Dis* 31: 55–61, 1998
24. Gattone VH, Cowley BDJ, Barash BD, Nagao S, Takahashi H, Yamaguchi T, Grantham JJ: Methylprednisolone retards the progression of inherited polycystic kidney disease in rodents. *Am J Kidney Dis* 25: 302–313, 1995